Zentrum für Technomathematik
Fachbereich 3 – Mathematik und Informatik

On the statistical distribution of elastic moduli polycrystals

Pavel Bobrov
Werner Wosniok

Report 10–02

Berichte aus der Technomathematik

Report 10–02 **April 2010**

On the statistical distribution of elastic moduli in polycrystals*

Pavel Bobrov
Institute of Statistics
University of Bremen
Bremen
Germany

file: DistElMod_V6.tex 14.01.2010

May 11, 2010

Abstract

A method for calculating the distributions of the components of stiffness and compliance tensors of cubic polycrystalite material from parameters of single crystals is developed. Their mathematical form is derived under the assumption of normal distributions for the members of the rotation group SO(3). Finally the impact of texture on the distributions of Young's modulus E, shear modulus G and Poisson's ratio ν analyzed.

1. The problem The elastic properties of polycrystalite material are described by the compliance tensor S_{ijkl} or the stiffness tensor C_{ijkl} $(i, j, k, l = 1, 2, 3)$ [1, 2, 3]. Because of the symmetry of strain and stress tensor, and for energetical considerations both tensors can be expressed by symmetric matrices S_{ij} and C_{ij} $(i, j = 1, 2, ..., 6)$, respectively, each containing 21 independent components [1]. In the sequel we focus on the compliance tensor, the components of which are termed elastic moduli.

For anisotropic crystals the symmetry properties of the various crystal systems reduce the number of independent matrix elements. As an example, there are only three independent elements for a cubic crystal system [2, 3].

*Paper prepared in the framework of the Sonderforschungsbereich 747 "Mikrokaltumformen - Prozesse, Charakterisierung, Optimierung", project B2 "Verteilungsbasierte Simulation", University of Bremen, supported by Deutsche Forschungsgemeinschaft

To describe a single crystal, an orthogonal coordinate system tightly connected to the crystal axes may be chosen. Such a system is called a crystal physical coordinate system. We choose the directions of the cube edges as axes for a cubic crystal system [3]. In this coordinate system the compliance tensor s_{ijkl} may be represented in matrix form as

$$\begin{pmatrix} s_{11} & s_{12} & s_{12} & 0 & 0 & 0 \\ & s_{11} & s_{12} & 0 & 0 & 0 \\ & & s_{11} & 0 & 0 & 0 \\ & & & s_{44} & 0 & 0 \\ & & & & s_{44} & 0 \\ & & & & & s_{44} \end{pmatrix} \tag{1}$$

where $s_{11} = s_{1111}$, $s_{12} = s_{1122}$ and $s_{44} = s_{1212}$.

Now we define an orthogonal coordinate system in the specimen. This coordinate system may be chosen arbitrarily. We use the RTN system [3], which is commonly used for sheets and foils.

We describe the orientation of a crystalite in a polycrystal by a rotation g, which maps the probenfest system on the crystal physical system. These rotations constitute the rotation group SO(3). For the tensor S_{ijkl} in the RTN system we have the tensor representation of the rotation group[1]:

$$S_{ijkl} = g_{ip} g_{jq} g_{km} g_{ln} s_{pqmn} \tag{2}$$

where g_{ij} denotes the components of the rotation matrix.

As crystalites in the polycrystal are randomly orientated, also the components g_{ij} show a random variation, which induces random variation in the values of the elastic moduli. If the orientations of the crystalite are uniformly distributed, the corresponding polycrystal is quasi isotropic. If a principal orientation exists, we have a texture.

This contribution considers the distributions of the matrix elements of the compliance tensor for a polycrystal that are induced by normal measures on SO(3).

2. Distributions on SO(3) The general theory for distributions on locally compact groups is dealt with in [6, 7]. We consider distributions $d\mu = f(g)dg$, $g \in$SO(3), where dg is an invariant measure on SO(3). If Rotation g is parametrized by Euler angles $g = g(\varphi_1, \theta, \varphi_2)$, $\theta \in [0, \pi]$ and $\varphi_1, \varphi_2 \in [-\pi, \pi)$ we have [4, 8]

$$dg = \frac{\sin\theta d\theta}{2} \frac{d\varphi_1}{2\pi} \frac{d\varphi_2}{2\pi}$$

[1] We sum over repeatedly occurring indices.

The texture function $f(g)$ [5], which depends on the orientation, may be expanded as a series of generalized spheric functions

$$f(g) = \sum_{l=0}^{\infty} \sum_{m,n=-l}^{l} C^l_{mn} T^l_{mn}(g)$$

If $f(g) = 1$, the polycrystal is quasi isotropic. For this case, the distribution of the elastic moduli of hexagonal polycrystals has been approximated by quadratic polynomials in [9].

An important distribution class on SO(3) is the class of normal distributions. We define these according to [10, 12] in the following way: a measure μ on SO(3) has a normal distribution, if μ is infinitely divisible and not idempotent, and if we have for each irreducible representation T_g of the group that

$$\int_G T_g d\mu(g) = \exp\left[\sum_{i,j} \alpha_{ij} A_i A_j + \sum_i \alpha_i A_i\right]$$

holds, where A_i are infinitesimal operators of this representation, (α_{ij}) is a positive definite symmetric matrix, and α_i are real numbers. If $\alpha_{ij} = 0$ for $i \neq j$, we have a canonical normal distribution [11] with analytical probability distribution

$$\begin{gathered} f(g) = \sum_{l=0}^{\infty}(2l+1)\exp[-l(l+1)p^2]\times \\ \times \sum_{m=-l}^{l} \exp[m^2(q^2-r^2)]\exp[-im(\varphi_1+\varphi_2)]P^l_{mm}(\cos\theta) \end{gathered} \tag{3}$$

Here, $P^l_{mm}(x)$ are Jacobian polynomials with parameters q, r, p. However, though we consider orientation distributions belonging to the family of canonical distributions, eq. (3) is not useful for our purpose.

Another way to derive the desired distributions lies in the application of Parthasarathy's [12] central limit theorem for the rotation group. We need some additional notation for this theorem. Let $g_n = \int_{\mathrm{SO}(3)} g d\mu_n(g)$ be the mean of the measure $\mu_n(g)$, $n = 1, 2, 3, ...$, μ_n^{*n} ($d\mu_2^{*2}(g) = \int_{\mathrm{SO}(3)} \mu_2(gg_1^{-1})d\mu_2(g_1)$) n-fold convolution μ_n and $\mu_n(SO(3)\backslash U_e)$ the value of the measure $\mu_n(g)$ outside the neighbourhood U_e of the null element e of the group.

A Central Limit Theorem for SO(3) (Parthasarathy). Let $\{\mu_n\}$ (n=1,2,3,...) be a sequence of distributions on SO(3), which converges to a degenerate distribution in e as $n \to \infty$. The sequence μ_n^{*n} of convolutions converges to a normal distribution if and only if for $n \to \infty$ holds

1. $n(1 - |g_n|) < \infty$

2. $n\mu_n(SO(3)\backslash U_e) \to 0$

With the additional condition $\lim_{n\to\infty} n(e - g_n) = A$ the parameters α_{ij} and α_i of the distribution μ_n^{*n} are given by

$$-A = \sum_{i=1}^{3}\sum_{j=1}^{3} \alpha_{ij} a_i a_j + \sum_{i=1}^{3} \alpha_i a_i$$

with $a_i = \lim_{t\to 0} \frac{g_i(t)-e}{t}$, where $g_i(t)$ are the one-parametric subgroups of SO(3).

3. Simulation of orientation distributions Due to the CLT we may specify an order $\mu_n(g)$. We use the concept of small rotations [13] for this purpose. The set of small rotations corresponds to a certain set of Euler angles:

$$\begin{cases} 1 - (e_z', e_z) = 1 - \cos\theta \le a \\ 1 - (e_x', e_x) = 1 - \cos\varphi_1 \cos\varphi_2 + \sin\varphi_1 \sin\varphi_2 \cos\theta \le b \\ 1 - (e_y', e_y) = 1 + \sin\varphi_1 \sin\varphi_2 - \cos\varphi_1 \cos\varphi_2 \cos\theta \le b \\ 0 \le a, b \ll 1 \end{cases} \tag{4}$$

Here, (e_x, e_y, e_z) form a basis before a small rotation and (e_x', e_y', e_z') thereafter. Given that $a, b \ll 1$, (4) simplifies to

$$\frac{\theta^2}{2} \le a \quad , \quad \frac{(\varphi_1 + \varphi_2)^2}{2} \le b$$

The set of small rotations now is represented by the region

$$\Pi(a, b) = \left\{ (\varphi_1, \theta, \varphi_2) : \ \theta \le \sqrt{2a} = \bar{a} \ , \ |\varphi_1 + \varphi_2| \le \sqrt{2b} = \bar{b} \right\}$$

The sequence of measures $d\mu_n = f_n(g)dg$, with dg denoting the invariant measure, f_n the rectangular distribution in $\Pi(a_n, b_n)$, $a_n = \bar{a}/\sqrt{n}$, $b_n = \bar{b}/\sqrt{n}$ and

$$f_n(\varphi_1, \theta, \varphi_2) = \begin{cases} \frac{2}{1-\cos a_n} \cdot \frac{4\pi^2}{b_n(4\pi - b_n)} & (\varphi_1, \theta, \varphi_2) \in \Pi(a_n, b_n) \\ 0 & (\varphi_1, \theta, \varphi_2) \notin \Pi(a_n, b_n) \end{cases} \tag{5}$$

corresponds to the sequence of convolutions

$$d\mu_n^{*n} = \left[\int_{SO(3)} dg_{n-1} f_n(g g_{n-1}^{-1}) \ldots \int_{SO(3)} dg_1 f_n(g_2 g_1^{-1}) f_n(g_1) \right] dg \ , \tag{6}$$

which converges for $t \to \infty$ to the canonical normal distribution on SO(3) with parameters $q^2 = \bar{a}^2/8$ and $r^2 = \bar{b}^2/6$ [13].

The realisation of the random variable g $\in$SO(3) with distribution 6) is the product of the small random rotations $g = g_1 g_2 ... g_n$, where $g_i = g(\varphi_1^i, \theta^i, \varphi_2^i)$ $\in$SO(3) with density (5). The Euler angles $(\varphi_1^i, \theta^i, \varphi_2^i)$ are given by [13]:

$$\varphi_1^i = \begin{cases} -(\pi + b_n) + \sqrt{b_n^2 + 2b_n(4\pi - b_n)\xi_1^i} \;; & \xi_1^i < \frac{3b_n}{2(4\pi - b_n)} \\ \left(\frac{b_n}{4} - \pi\right) + \frac{4\pi - b_n}{2}\xi_1^i \;; & \frac{3b_n}{2(4\pi - b_n)} \leq \xi_1^i < 1 - \frac{3b_n}{2(4\pi - b_n)} \\ (\pi + b_n) - \sqrt{b_n^2 + 2b_n(4\pi - b_n)(1 - \xi_1^i)} \;; & 1 - \frac{3b_n}{2(4\pi - b_n)} \leq \xi_1^i \end{cases}$$

$$\theta^i = \arccos\left(1 - \xi_2^i(1 - \cos a_n)\right) \tag{7}$$

$$\varphi_2^i = \begin{cases} \pi - \xi_3^i(b_n + \pi + \varphi_1^i) \;; & -\pi \leq \varphi_1^i < b_n - \pi \\ -\varphi_1^i + 2b_n\left(\xi_3^i - \frac{1}{2}\right) \;; & |\varphi_1^i| \leq \pi - b_n \\ -\pi + \xi_3^i(b_n + \pi - \varphi_1^i) \;; & \pi - b_n < \varphi_1^i \leq \pi \end{cases}$$

where ξ_1^i, ξ_2^i, ξ_3^i are independent and uniformly distributed in [0,1].

In [13] it was shown that convolution parameters $n \geq 20$ generate a good agreement of μ_n^{*n} with a normal distribution with density given in (3).

The distribution of crystalite orientations may be modelled by Monte Carlo simulation and the material parameters of interest are subsequently derived from these. Figure 1 shows the distribution of the projection of the nutation angle θ on the sphere for selected values of $\bar{a} = 0.2$, $\bar{b} = 0.5$ and n. This distribution results from 10000 realizations. If the polycrystal material has a certain texture g_0 with main orientation different from the cube coordinate edges, the resulting normal distribution (in the sense of SO(3)) of the nutation angle is shifted towards this actual orientation.

4. Results. Equation (2) leads to the tensor (1)

$$S_{11} = s_{11} - 2\mu^s \left(g_{11}^2 g_{21}^2 + g_{11}^2 g_{31}^2 + g_{21}^2 g_{31}^2\right)$$

$$S_{12} = s_{12} + \mu^s \left(g_{11}^2 g_{12}^2 + g_{21}^2 g_{22}^2 + g_{31}^2 g_{32}^2\right)$$

$$S_{44} = s_{44} + 4\mu^s \left(g_{12}^2 g_{13}^2 + g_{22}^2 g_{23}^2 + g_{32}^2 g_{33}^2\right) \tag{8}$$

$$S_{14} = 2\mu^s (g_{11}^2 g_{12} g_{13} + g_{21}^2 g_{22} g_{23} + g_{31}^2 g_{32} g_{33})$$

$$S_{16} = 2\mu^s (g_{11}^3 g_{12} + g_{21}^3 g_{22} + g_{31}^3 g_{32})$$

where $\mu^s = s_{11} - s_{12} - s_{44}/2$ is the measure of anisotrophy[2]. [14]. If the elements of the rotation matrix g_{ij} is parametrized by Euler angles, the equations (8) may be given as

$$S_{ij} = s_{ij} + \mu^s C_{ij} \Lambda_{ij}(\varphi_1, \theta, \varphi_2)$$

Here, we have a normal distribution of $g = g(\varphi_1, \theta, \varphi_2)$ on SO(3) around a preferred orientation $g_0 = g(\varphi_1^0, \theta^0, \varphi_2^0)$.

We consider aluminium as example of a polycrystal material with $s_{11} = 1.57$, $s_{12} = -0.57$ and $s_{44} = 3.51$ (all units: 10^{-11} GPa^{-1}) [15] and a rolling texture (1,1,2)[$\bar{1}$,$\bar{1}$,1] [14, 16]. The principal representation matrix for this orientation is

$$\begin{pmatrix} -\frac{1}{\sqrt{3}} & \frac{1}{\sqrt{2}} & \frac{1}{\sqrt{6}} \\ -\frac{1}{\sqrt{3}} & -\frac{1}{\sqrt{2}} & \frac{1}{\sqrt{6}} \\ \frac{1}{\sqrt{3}} & 0 & \frac{\sqrt{2}}{\sqrt{3}} \end{pmatrix} \tag{9}$$

The parameters $\bar{a}$ and $\bar{b}$ define the strength of the texture: smaller parameters indicate crystallites lying closer to the main orientation. Figures 2 and 3 allow comparing the dispersion of the nutation angle corresponding to various $\bar{a}$ and $\bar{b}$ for the same given RTN texture. Obviously the dispersion of Λ_{ij} and S_{ij} depend on the strength of the texture and increase with its decrease.

For further insight into the relation between $\bar{a}$ and $\bar{b}$ and the corresponding distributions of the various S_{ij} quantities we did Monte Carlo simulations

[2] All other S_{ij} result from cyclical re-arrangement of indices, e.g.

$$S_{66} = s_{44} + 4\mu^s \left(g_{11}^2 g_{12}^2 + g_{21}^2 g_{22}^2 + g_{31}^2 g_{32}^2\right)$$

with 10000 realizations for several values of $(\bar{a}, \bar{b})$. The resulting S_{ij} distributions are shown in Figures 4 - 11.

Obviously, with increasing parameters $\bar{a}$ and $\bar{b}$ the set of small rotations $\Pi(a, b)$ increases to the full set $\{0 \leq \theta \leq \pi;\ -\pi \leq \varphi_1; \varphi_2 \leq \pi\}$ and the distribution of orientations becomes a uniform distribution on SO(3).

Using the distributions of the elastic moduli we are able to derive the distributions of the Young's modulus in arbitrary directions $E_{\alpha\alpha}$, of the Shear modulus $G_{\alpha\alpha}$ or of Poisson's ratio $\nu_{\alpha\alpha}$ [14]. As an example we have

$$E_{WW} = 1/S_{11} \quad , \quad G_{WQ} = 1/S_{44} \quad , \quad \nu_{WQ} = -S_{12}/S_{11}$$

Figures 12-17 display parameter distributions under two different textures, each obtained for $\bar{a} = 0.15$, $\bar{b} = 0.3$ and $n = 100$, based on 10000 Monte Carlo realizations. Figures in the left column contain E_{WW}, G_{WQ} and ν_{WQ} for the texture (1,1,2)[$\bar{1}$,$\bar{1}$,1] from above, while the right column of figures refers to the texture (1,1,0)[1,$\bar{1}$,2]. The Young's modulus in arbitrary directions α in the rolling plane can be calculated according to the formulae

$$S_{\alpha\alpha} = S_{11} \cos^4 \alpha + (2S_{12} + S_{66}) \cos^2 \alpha \sin^2 \alpha + S_{22} \sin^4 \alpha$$

and $E_{\alpha\alpha} = 1/S_{\alpha\alpha}$. Figure 18 shows the dependence of mean and quantiles of the Young's modulus distribution on the angle α between the rolling direction and direction concerned for the texture (1,1,2)[$\bar{1}$,$\bar{1}$,1]. The dependence was obtained for $\bar{a} = 0.2$, $\bar{b} = 0.3$ and $n = 100$, based on 2000 Monte Carlo realizations.

Having determined the distributions of interest by Monte Carlo simulation we can derive descriptive quantities for this distribution. As an example, we have for the Shear modulus in the left column of Figures 12-17 (all values in GPa)

Mean	SD	Min	Q1	Median	Q3	Max
26.54	0.40	25.08	26.27	26.54	26.81	27.87

Figure 19 displays the distribution of $E_{QQ} = 1/S_{22}$, again for the texture (1,1,2)[$\bar{1}, \bar{1}, 1$].

5. Discussion. In the preceding sections we showed a method for deriving the distribution of the elastic moduli S_{ij} assuming a normal distribution for the orientation of single crystalites in a textured polycrystal. As the S_{ij} are complicated functions of the Euler angles, we cannot describe their distributions by simple standard distributions. However, we can obtain all characterizing quantities of these distributions up to a histogram or density estimate of the complete distribution in a relatively simple way. As additionally all distributions have compact support, a first approximation by polynomials or mixtures of these may be considered. For strongly textured material ($\bar{a} \leq 0.2$ and $\bar{b} \leq 0.3$) the distributions of some S_{ij} may well be approximated by normal or log-normal distributions. A more precise description of the S_{ij} distributions can be obtained by mixtures of distribution. This aspect, however, lies outside the scope of this contribution.

A further problem is the determination of the parameters q and r (corresponding to $\bar{a}$ and $\bar{b}$) of the canonical normal distribution (3) of the experimental material. These can be derived from the pole figures [11].

All distributions presented here were obtained while neglecting possible correlations between properties of different crystalites. Including such correlations into the consideration, which is especially necessary for analyzing multiphase polycrystals, will be a further step.

The method employed here cannot only be used for the calculation of elastic parameters, but also for the calculation of further material parameters that allow representation by tensor quantities.

References

[1] W. Voigt: Lehrbuch der Kristallphysik (Teubner), Leipzig-Berlin (1928).

[2] T. Šermegor: Die Elastizitätstheorie mikroinhomogener Medien, Nauka, Moskau (1977).

[3] H.-J. Bunge: Mathematische Methoden der Texturanalyse, Akademie-Verlag, Berlin (1969).

[4] I. Gelfand, R. Minlos, Z. Shapiro: Representations of the Rotation and Lorentz Groups and their Applications, Pergamon Press, Oxford - London - New York - Paris (1963).

[5] A. Wiglin: Physics of the Solid State 2(1960) 2463.

[6] U. Grenander: Probability on algebraic structures, Almquist & Wiksell, Stockholm (1963).

[7] H. Heyer: Probability Measures on Locally Compact Groups, Springer-Verlag, Berlin - Heidelberg - New York (1977).

[8] A. Weil: L'integration dans les groupes topologiques et ses applications, Hermann, Paris (1965).

[9] V. Bykov, S. Volkov, N. Klinskih: Journal of Applied Mechanics and Technical Physics 4(1960) 69.

[10] T. Savyolova: Industrial Laboratory 50(1984) 468.

[11] T. Savyolova: Textures and Microstructures 22(1993) 17.

[12] K. Parthasarathy: Theory of Probabilities and its Application 9(1964) 273.

[13] M. Borovkov, T. Savyolova: Industrial Laboratory 68(2002) 16.

[14] D.A.G Bruggeman: Zeitschrift für Physik A Hadrons and Nuclei 92(1934) 561.

[15] I. Francevič, F. Voronov, S. Bakuta: Elastizitätskonstanten und Elastizitätsmoduln von Metallen und Nichtmetallen, Naukova Dumka, Kiev (1982).

[16] G. Wasserman, J. Grewen: Texturen metallischer Werkstoffe, Springer-Verlag, Berlin - Göttingen - Heidelberg (1962).

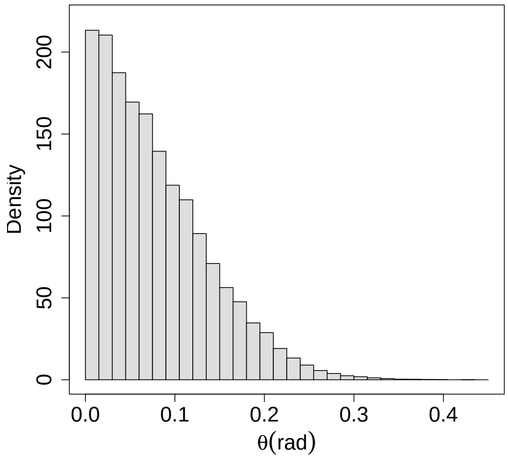

Figure 1. *Histogram of the distribution of the nutation angle* θ *for* $\bar{a} = 0.2$, $\bar{b} = 0.5$ *and* $n = 50$

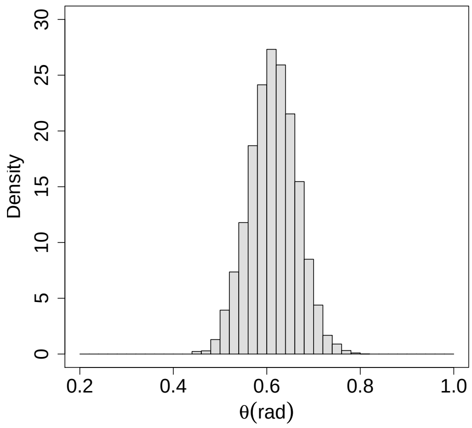

Figure 2. *Histogram of the distribution of the nutation angle* θ *for* $\bar{a} = 0.1$, $\bar{b} = 0.2$ *and* $n = 100$, *given a RTN texture*

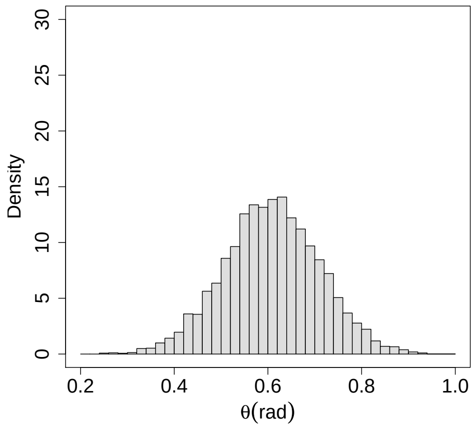

Figure 3. *Histogram of the distribution of the nutation angle*θ *for* $\bar{a} = 0.2$, $\bar{b} = 0.4$ *and* $n = 100$, *given a RTN texture*

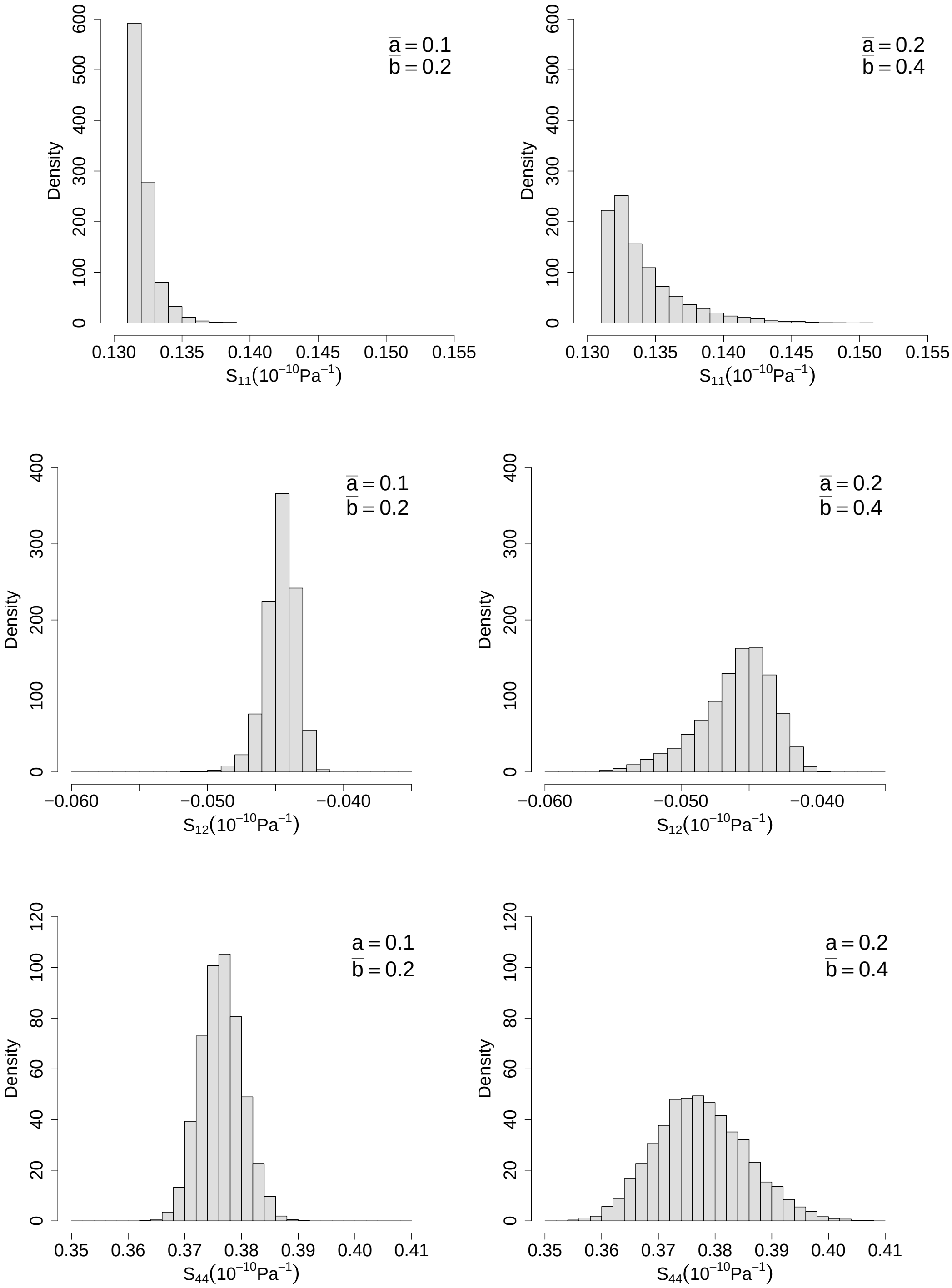
ā = 0.1
b̄ = 0.2
Density
S11(10−10Pa−1)
ā = 0.2
b̄ = 0.4
Density
S11(10−10Pa−1)
ā = 0.1
b̄ = 0.2
Density
S12(10−10Pa−1)
ā = 0.2
b̄ = 0.4
Density
S12(10−10Pa−1)
ā = 0.1
b̄ = 0.2
Density
S44(10−10Pa−1)
ā = 0.2
b̄ = 0.4
Density
S44(10−10Pa−1)

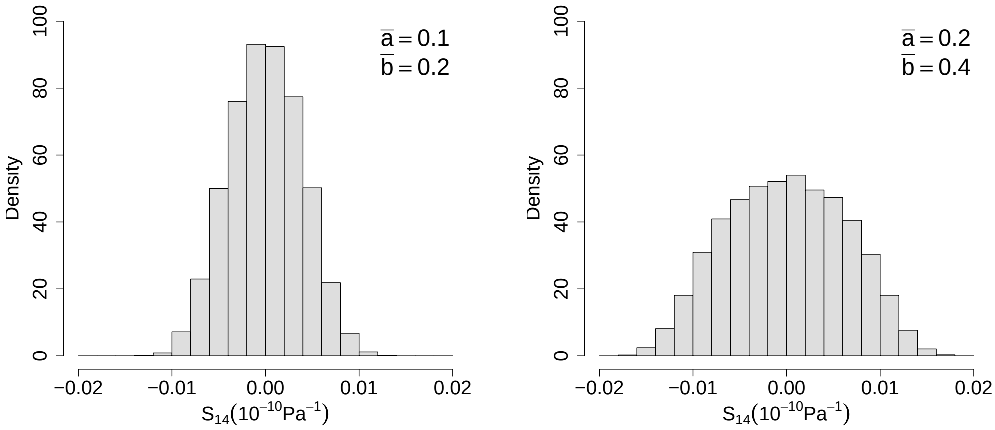

Figures 4-11. *Distributions of various S_{ij} for a set of $\bar{a}$ und $\bar{b}$ values.*

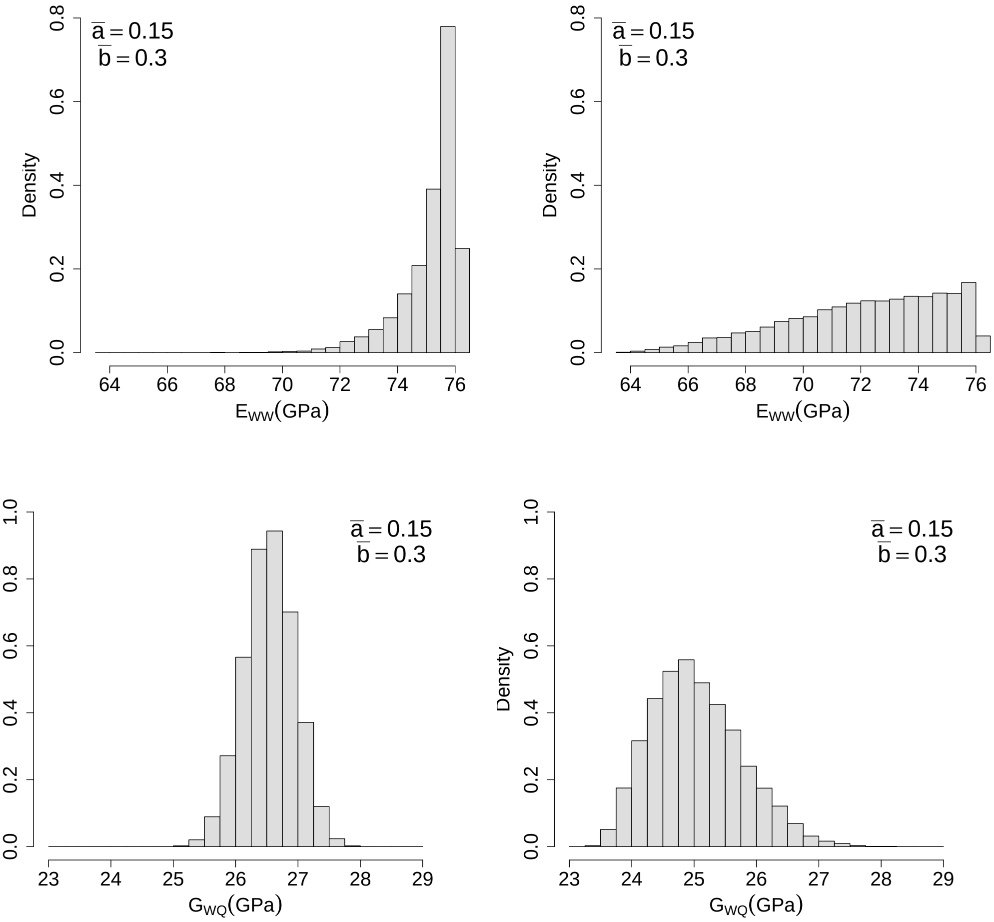

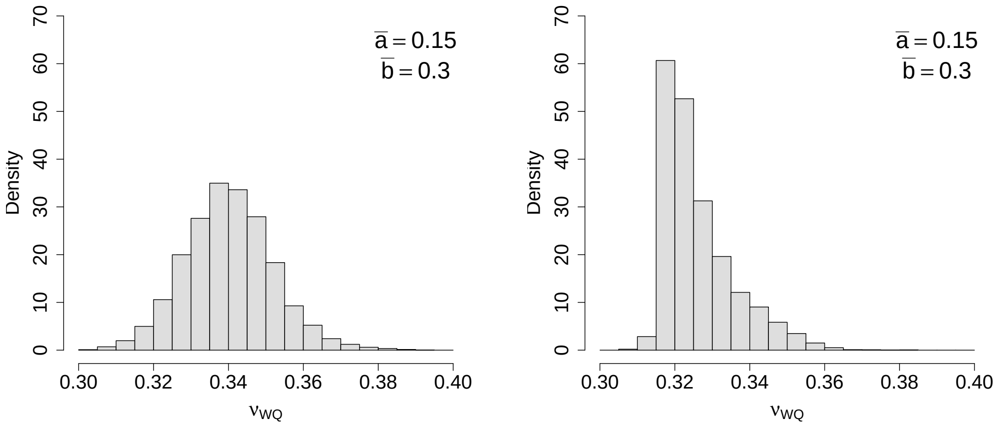

Figure 12-17. *Histogram of the distribution of various elastic parameters for* $\bar{a} = 0.15$, $\bar{b} = 0.3$ *and* $n = 100$. *Left column: texture (1,1,2)[$\bar{1}$,$\bar{1}$,1], right column: texture (1,1,0)[1,$\bar{1}$,2]*

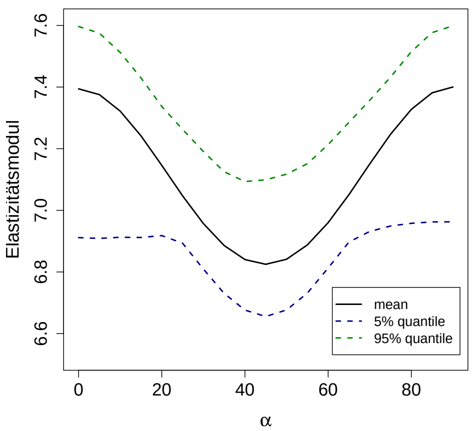

Figure 18. *Diagram of the Young's modulus* $E_{\alpha\alpha} = 1/S_{\alpha\alpha}$ *for* $\bar{a} = 0.2$, $\bar{b} = 0.3$ *and* $n = 100$ *with the quantiles;* $\alpha \in [0, \pi/2]$

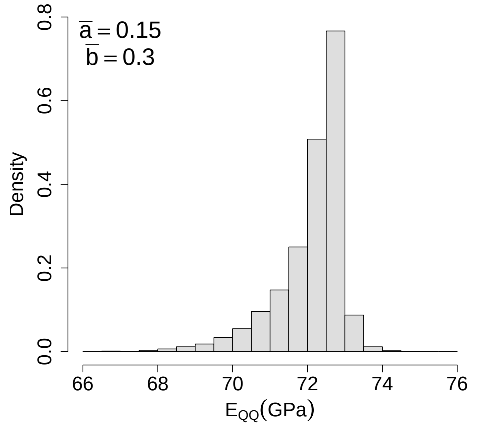

Figure 19. *Histogram of the distribution of the distribution of the Young's modulus* $E_{QQ} = 1/S_{22}$ *for* $\bar{a} = 0.15$, $\bar{b} = 0.3$ *and* $n = 100$